

# NF- $\kappa$ B-induced oxidative stress contributes to mitochondrial and cardiac dysfunction in type II diabetes

Nithya Mariappan<sup>1</sup>, Carrie M. Elks<sup>1</sup>, Srinivas Srinamula<sup>1</sup>, Anuradha Guggilam<sup>1</sup>, Zhizhen Liu<sup>1,2</sup>, Olga Borkhsenius<sup>1</sup>, and Joseph Francis<sup>1\*</sup>

<sup>1</sup>Department of Comparative Biomedical Sciences, Louisiana State University School of Veterinary Medicine, Louisiana State University, Baton Rouge, LA 70803, USA; and

<sup>2</sup>Department of Biochemistry and Molecular Biology, Shanxi Medical University, Taiyuan 030001, China

Received 1 May 2009; revised 28 August 2009; accepted 1 September 2009; online publish-ahead-of-print 3 September 2009

Time for primary review: 25 days

**Aims** Inflammatory molecules and their transcription factor, nuclear factor kappa-B (NF- $\kappa$ B), are thought to play important roles in diabetes-induced cardiac dysfunction. Here, we investigated the effects of pyrrolidine dithiocarbamate (PDTC), a NF- $\kappa$ B inhibitor, in diabetic mice.

**Methods and results** Obese *db/db* mice and heterozygous lean mice ( $n = 8$ ) were allowed free access to drinking water (control) or water containing PDTC (100 mg/kg) for 20 weeks. Left ventricular (LV) function was measured using echocardiography at baseline and at study end. Mice were sacrificed and LV removed for gene expression, biochemical, immunofluorescence, and mitochondrial assays. LV and mitochondrial reactive oxygen species (ROS), superoxide and peroxynitrite were measured using electron spin resonance spectroscopy. Enhanced NF- $\kappa$ B activity in *db/db* mice was associated with increased oxidative stress as demonstrated by increased ROS, superoxide, and peroxynitrite production, and increased NF- $\kappa$ B, gp91phox, and Nox1 expression; PDTC ameliorated these effects. Mitochondrial free radical production and structural damage were higher in the *db/db* group than in the control, *db/db* PDTC, and PDTC-treated heterozygous animal groups.

**Conclusion** This study demonstrates that NF- $\kappa$ B blockade with PDTC mitigates oxidative stress and improves mitochondrial structural integrity directly, through down-regulation of increased oxygen-free radicals, thereby increasing ATP synthesis and thus restoring cardiac function in type II diabetes.

**Keywords** Type II diabetes • NF- $\kappa$ B • Mitochondria • Oxidative stress • Free radicals

## 1. Introduction

Diabetes mellitus (DM) is a disease of epidemic proportion affecting approximately 24 million Americans.<sup>1</sup> An additional 50 million Americans have cardiometabolic syndrome,<sup>2</sup> which, if left untreated, can lead to type II DM and cardiovascular disease. DM is rarely a 'stand-alone' disease and is often accompanied by other sequelae, including obesity, hypertension, and hyperlipidaemia;<sup>3,4</sup> all of which contribute to the initiation and progression of cardiovascular disease. One of the major hypotheses to explain the onset of diabetic complications is a

DM-induced increase in oxidative stress in the absence of the counterbalancing effects of endogenous antioxidants. Several previous investigations have examined the role of oxidative stress in the development of DM-mediated disorders, possibly via the formation of free radicals.<sup>5,6</sup> Reactive oxygen species (ROS), such as superoxide, generated by high glucose concentrations are also considered a causal link between hyperglycaemia and other metabolic abnormalities in the development of many complications of DM.<sup>7</sup> Hence, one of the primary goals in the management of DM is the protection of the end organs against its deleterious effects.

\* Corresponding author. Tel: +1 225 578 9752, Fax: +1 225 578 9895, Email: jfrancis@lsu.edu

Nitric oxide (NO) produced in endothelial cells and cardiomyocytes is important in the regulation of cardiac function.<sup>8,9</sup> However, excess NO can be toxic; its toxic effects are not generally due to the NO molecule itself, but to its reaction with superoxide to form the highly reactive oxidant, peroxynitrite.<sup>10</sup> The reaction of peroxynitrite with various macromolecules can influence normal cellular function. Tyrosine nitration by peroxynitrite to form 3-nitrotyrosine (3-NT), an indirect indicator of peroxynitrite formation, can lead to protein dysfunction.<sup>10,11</sup> Peroxynitrite can also oxidize sulfhydryl groups in enzymes critical to the mitochondrial electron transport chain (ETC).<sup>12</sup> Cardiac contractile dysfunction is believed to be caused, in part, by the effects of peroxynitrite on creatine kinase activity in myofibrils.<sup>10,11</sup> Peroxynitrite generation also decreases the NO available for G-protein stimulation and vasodilation and can deplete cellular antioxidants, thus contributing to endothelial dysfunction.<sup>9,10</sup> Since it is known to have various effects on the heart, and to be produced in DM, we measured peroxynitrite formation indirectly by measuring 3-NT levels.

Recent findings suggest that proinflammatory cytokines (PIC), like tumour necrosis factor- $\alpha$  (TNF- $\alpha$ ), interleukin-1 beta (IL-1 $\beta$ ) and IL-6, play important roles in the pathophysiology of heart disease.<sup>13,14</sup> Recent findings from our laboratory suggest that chronic TNF- $\alpha$  administration induces cardiac damage and mitochondrial dysfunction.<sup>15,16</sup> Nuclear factor-kappa B (NF- $\kappa$ B), which is involved in PIC production and in the induction of ROS-mediated NF- $\kappa$ B activation,<sup>17,18</sup> may be important in cardiovascular and other disease states.<sup>19</sup> An understanding of the role of NF- $\kappa$ B in altering redox balance, and its contribution to cardiac damage at the mitochondrial level in type II DM is crucial.

We recently showed that blockade of NF- $\kappa$ B, the transcription factor for TNF- $\alpha$ , with pyrrolidine dithiocarbamate (PDTC) attenuates hypertensive response and renal damage in spontaneously hypertensive rats<sup>20</sup> and in obese Zucker rats.<sup>21</sup> PDTC is a dithiocarbamate with both antioxidant and pro-oxidant properties. The antioxidant properties of PDTC, however, may be restricted to only certain cell types.<sup>22,23</sup> Brennan and O'Neill have postulated that each pathway to NF- $\kappa$ B in a given cell type should be treated as a distinct one, with it being inappropriate to assume that the effects of oxidants and antioxidants on NF- $\kappa$ B are cell-independent and always due to redox modulation.<sup>24</sup> Although NF- $\kappa$ B inhibition by PDTC has often been attributed to its free-radical scavenging properties, PDTC has been demonstrated to exert its inhibitory effect on NF- $\kappa$ B through direct oxidation of the thiols of NF- $\kappa$ B.<sup>24,25</sup>

Mitochondrial dysfunction is prominent in most cardiovascular diseases.<sup>16,26</sup> Under physiological conditions, the ETC in mitochondria is a major producer of superoxide, while under pathological conditions, defects in mitochondrial activity lead to an overwhelming production of superoxide.<sup>27</sup> In diabetes, intracellular glucose is higher; therefore, more glucose can be oxidized by the Krebs cycle.<sup>28</sup> As a result of this metabolic alteration, more electron donors enter the ETC. The voltage across the mitochondrial membrane increases to a threshold point, where electron transfer inside complex III becomes blocked,<sup>29</sup> causing a backup of electrons, and decreased complex III activity. Impaired electron transport, in turn, leads to decreased ATP production, increased

formation of toxic-free radicals (primarily superoxide), and altered redox status.<sup>16</sup> Although oxidative stress and mitochondrial dysfunction are evident in several pathophysiological states, the role played by NF- $\kappa$ B in inducing mitochondrial ROS production in DM is not known. More importantly, it is not known whether NF- $\kappa$ B is found in the mitochondria and contributes to this increased ROS within the mitochondria, thereby contributing to cardiac dysfunction. The results from this study will help us elucidate the mechanisms by which NF- $\kappa$ B may induce mitochondrial redox imbalance in DM and will lead to a better understanding of the disease process, which might lead to new and effective strategies for cardioprotection in DM.

## 2. Methods

Detailed descriptions of methodologies can be found in the accompanying Supplementary material online.

### 2.1 Animals

Adult male obese *db/db* mice ( $n = 16$ ) and heterozygous lean control mice ( $n = 16$ ) weighing 28–30 g were used for the study. Animals were housed in temperature ( $23 \pm 2^\circ\text{C}$ ) and light-controlled (12 h light/dark cycle) animal quarters; standard rodent chow and water were provided *ad libitum*. This study conforms with the Guide for the Care and Use of Laboratory Animals published by the US National Institutes of Health (NIH Publication no. 85-23, revised 1996). All animal experimental protocols were approved by the Louisiana State University Institutional Animal Care and Use Committee (protocol number 09-008).

### 2.2 Experimental design

At 12 weeks of age, diabetic *db/db* mice were markedly obese and hyperglycaemic relative to heterozygous controls. To determine whether NF- $\kappa$ B blockade would protect against cardiac damage, appropriate groups ( $n = 8$  each) of mice were treated for 20 weeks, from age 12 to 32 weeks, with 100 mg/kg/day PDTC in drinking water. Control animals were given access to tap water *ad libitum*. Animals were treated for 20 weeks, since cardiac hypertrophy becomes evident at  $\sim 30$  weeks of age in obese animals. After 20 weeks of treatment, left ventricular (LV) function was measured using echocardiography; subsequently, mice were sacrificed by carbon dioxide inhalation and the LV was removed for gene expression, biochemical and immunofluorescence studies. Electron paramagnetic resonance (EPR) spectroscopy was used to measure free radicals in the cytosolic and mitochondrial fractions. The structural integrity of mitochondrial membranes was measured using swelling assay and transmission electron microscopy (TEM) analysis.

### 2.3 Echocardiography

Echocardiography was performed as previously described.<sup>30</sup>

### 2.4 Measurement of plasma cytokine and lipid levels

TNF- $\alpha$  and IL-6 concentrations in mouse plasma were determined with commercially available kits, according to the manufacturer's protocols (Biosource). Levels of total cholesterol, high-density lipoprotein (HDL-c), and very low-density lipoprotein (VLDL-c) in plasma were quantified by a kit method (BioVision, Mountain View, CA, USA) as per the manufacturer's instructions.

## 2.5 Determination of glutathione (GSH)/glutathione disulfide (GSSG) ratio

GSH and GSSG concentrations were determined in LV tissue by the use of a commercially available kit (Cayman Chemicals), as described previously.<sup>15,16</sup>

## 2.6 RNA isolation and real-time RT-PCR

Total RNA extraction, cDNA synthesis, and real-time RT-PCR were performed as previously described.<sup>15,20</sup>

## 2.7 Western blotting

Protein expression in mitochondria was analysed by western blotting as previously described,<sup>20</sup> using anti-p50, anti-ANT, anti-VDAC, and anti-Nox1 antibodies (Santa Cruz Biotechnology).

## 2.8 LV total ROS, O<sub>2</sub><sup>•-</sup>, and OONO<sup>-</sup> production

Total ROS, O<sub>2</sub><sup>•-</sup>, and OONO<sup>-</sup> production in the heart tissues were measured by EPR using the spin probes 1-hydroxy-3-methoxycarbonyl-2, 2, 5, 5-tetramethylpyrrolidine and 1-hydroxy-3-carboxypyrrolidine as described previously.<sup>16</sup>

## 2.9 Immunofluorescence

Immunofluorescence detection of 3-NT was performed as described previously,<sup>31</sup> with minor modifications (see Supplementary material online).

## 2.10 Quantification of NF-κB p65 activity

The NF-κB/p65 Active ELISA (Active Motif, USA) kit was used to measure the binding activity of free NF-κB p65 in nuclear extracts. The analysis was done using a sandwich ELISA method, according to the manufacturer's instructions.

## 2.11 Isolation of LV mitochondria

LV mitochondria were isolated by differential centrifugation of heart homogenates as described previously.<sup>15,16</sup> Mitochondrial purity was determined by western blotting with anti-VDAC and anti-ANT antibodies and by TEM.

## 2.12 Mitochondrial swelling assay

For assessment of mitochondrial permeability transition pore opening, mitochondrial swelling was measured.<sup>15</sup> Purity of mitochondria was measured using electron microscopy and western blot for the mitochondrial markers ANT and VDAC.

## 2.13 Ultrastructural studies

LV and isolated mitochondrial pellets were immediately fixed in a 1.25% solution of glutaraldehyde and 2% paraformaldehyde in 0.1 M sodium cacodylate buffer (pH 7.4). Pellets were then fixed in a 1% solution of osmium tetroxide. The fixed mitochondria were embedded in Epon-Araldite. Ultrathin sections (85 nm) were obtained using MT XL, RMC product, stained with uranyl acetate, and lead citrate and examined in a Joel JEM 1011 TEM at 80 kV accelerating voltage.

## 2.14 Mitochondrial total ROS, O<sub>2</sub><sup>•-</sup>, and H<sub>2</sub>O<sub>2</sub> production

ROS, O<sub>2</sub><sup>•-</sup>, and H<sub>2</sub>O<sub>2</sub> production rates in mitochondria were measured using EPR as described previously.<sup>16</sup>

## 2.15 Mitochondrial complex III enzymatic activity

Measurement of mitochondrial complex III enzymatic activity was performed as previously described.<sup>16</sup>

## 2.16 Measurement of ATP levels and ATP/ADP ratio

ATP production levels and ATP/ADP ratio were quantified in isolated mitochondria using a commercially available kit (BioVision) as described previously.<sup>16</sup> Briefly, tissues were lysed to free ATP into medium containing luciferase and luciferin, which produces light in the presence of ATP. The light emission is proportional to the amount of ATP present.

## 2.17 Statistical analyses

Data were analysed by ANOVA, followed Bonferroni's multiple comparison tests.  $P \leq 0.05$  was considered significant.

# 3. Results

## 3.1 Body weights and heart weights of animals

No differences in heart weight to body weight (HW to BW) ratios were noted between hz control and hz + PDTC animals ( $3.82 \pm 0.04$  and  $4.11 \pm 0.07$  mg/g, respectively). As expected, obese *db/db* mice exhibited significantly lower HW to BW ratios when compared with age-matched lean controls ( $2.78 \pm 0.02$  and  $3.82 \pm 0.04$  mg/g, respectively,  $P < 0.05$ ); HW to BW ratios were also lower in *db/db* + PDTC mice ( $2.95 \pm 0.06$  mg/g). The decreased ratios seen in both *db/db* groups was due to the significantly higher body weights of these animals.

## 3.2 Echocardiography

When compared with control animals, untreated obese *db/db* mice had progressive increases in LV end-diastolic dimension (LVD) and LV end-systolic dimension (LVS) and decreases in fractional shortening (FS%) measurements (Table 1). Additionally, *db/db* treated with PDTC and heterozygous lean control mice exhibited significant decreases in LVD and LVS and increases in FS%. These results indicate preservation of cardiac function in obese *db/db* mice treated with a NF-κB blocker.

## 3.3 Circulating levels of TNF-α and IL-6, and plasma lipids

Untreated obese *db/db* mice had increased circulating levels of TNF-α and IL-6 (Table 2); these increases were prevented by PDTC treatment. Plasma levels of total cholesterol and VLDL-c were significantly higher and HDL-c levels were significantly lower in *db/db* obese mice than hz controls (Table 2); PDTC restored HDL to near control levels. A similar trend was observed when the hz PDTC-treated group was compared with the obese *db/db* group.

## 3.4 Glutathione content of LV

LV GSH (Figure 1A) and GSH/GSSG ratio (Figure 1B) in obese *db/db* mice were decreased ( $5.84 \pm 0.09$  and  $2.86 \pm 0.20$  nmol/mg

**Table 1** Echocardiography data for all experimental groups at study end

Parameter	hz Control	db/db	db/db + PDTC	hz + PDTC
IVSD (mm)	0.65 ± 0.05	0.64 ± 0.04	0.72 ± 0.03	0.78 ± 0.03
IVSS (mm)	1.25 ± 0.06	1.10 ± 0.01	1.12 ± 0.02	1.17 ± 0.04
LVD (mm)	3.70 ± 0.17 <sup>#</sup>	4.89 ± 0.01 <sup>*,†,‡</sup>	4.10 ± 0.07 <sup>#</sup>	4.08 ± 0.08 <sup>#</sup>
LVS (mm)	2.45 ± 0.05 <sup>#</sup>	3.17 ± 0.08 <sup>*,‡</sup>	2.62 ± 0.12	2.58 ± 0.01 <sup>#</sup>
PWD (mm)	0.69 ± 0.02	0.69 ± 0.03	0.74 ± 0.01	0.84 ± 0.04
PWS (mm)	1.12 ± 0.05	1.19 ± 0.02	1.33 ± 0.03	1.26 ± 0.03
FS%	36.11 ± 1.06 <sup>#</sup>	23.69 ± 0.39 <sup>*,†,‡</sup>	35.10 ± 0.31 <sup>#</sup>	34.10 ± 0.20 <sup>#</sup>
HR	437 ± 7.70	420 ± 10.2	437 ± 10.0	431 ± 5.21

Echocardiographic analysis revealed that both left ventricular diastolic (LVD) and systolic (LVS) dimensions were significantly greater and FS% measurements were lower in *db/db* mice, whereas *db/db* treated with PDTC and heterozygous lean control mice exhibited significant decreases in LVD, LVS and increases in FS%. Values are expressed as means ± SEM.  $P < 0.05$  = significant. Values presented are means ± SEM.

\* $P < 0.05$  vs. control.

<sup>#</sup> $P < 0.05$  vs. *db/db*.

<sup>†</sup> $P < 0.05$  vs. *db/db* PDTC.

<sup>‡</sup> $P < 0.05$  vs. hz PDTC.

**Table 2** Selected metabolic parameters for all groups at study end

Parameter	hz Control	db/db	db/db + PDTC	hz + PDTC
Plasma TNF- $\alpha$ (pg/mL)	5.0 ± 0.10 <sup>#,‡</sup>	21.6 ± 1.1 <sup>*,†,‡</sup>	3.0 ± 0.3 <sup>#</sup>	4.5 ± 0.7 <sup>*,#</sup>
Plasma IL-6 (pg/mL)	5.74 ± 0.11 <sup>#,‡</sup>	25.86 ± 1.59 <sup>*,†,‡</sup>	10.43 ± 1.74 <sup>#</sup>	13.72 ± 1.68 <sup>*,#</sup>
Cholesterol (mmol/L)	1.61 ± 0.02 <sup>#</sup>	2.58 ± 0.07 <sup>*,†,‡</sup>	1.46 ± 0.09 <sup>#</sup>	1.59 ± 0.08 <sup>#</sup>
HDL-c (mmol/L)	0.02 ± 0.002 <sup>#</sup>	0.009 ± 0.00 <sup>*,†,‡</sup>	0.019 ± 0.002 <sup>#</sup>	0.028 ± 0.005 <sup>#</sup>
LDL-c (mmol/L)	0.19 ± 0.027 <sup>#</sup>	0.62 ± 0.02 <sup>*,†,‡</sup>	0.28 ± 0.01 <sup>#</sup>	0.10 ± 0.017 <sup>#</sup>

Values are expressed as means ± SEM. Statistical analysis was performed.  $P \leq 0.05$  were considered significant.

\* $P < 0.05$  vs. control.

<sup>#</sup> $P < 0.05$  vs. *db/db*.

<sup>†</sup> $P < 0.05$  vs. *db/db* PDTC.

<sup>‡</sup> $P < 0.05$  vs. hz PDTC.

protein and  $11.46 \pm 2.29$  and  $6.31 \pm 0.31$  nmol/mg protein, respectively;  $P < 0.05$ ) compared with the control group; LV GSH and GSSG levels of *db/db* + PDTC mice were restored to that of control levels ( $9.35 \pm 0.38$  and  $4.52 \pm 0.13$  nmol/mg protein, respectively). A significant increase in GSH and GSSG content was seen in the hz mice treated with PDTC ( $1.96 \pm 0.01$  and  $2.30 \pm 0.01$  nmol/mg protein, respectively) when compared with the *db/db* animals ( $P < 0.05$ ).

### 3.5 Gene and protein expression studies

Gene and protein expression of Nox1 and gp91phox subunits in LV tissue were measured using real-time RT-PCR and western blotting. Untreated obese *db/db* mice had increased LV mRNA levels of gp91phox (Figure 2A) and Nox1 (Figure 2B); these increases were prevented by PDTC treatment.

### 3.6 Total LV ROS and O<sub>2</sub><sup>-</sup> production

Superoxide and total ROS production rates in LV tissues appear in Figure 2C and D. The rates of ROS and superoxide production in untreated obese *db/db* animals were significantly higher than

those of the heterozygous control animals. PDTC treatment of *db/db* mice inhibited the increased rate of ROS production as well as the accumulation of superoxide anions ( $P < 0.05$  for all). The same trend was observed when the heterozygous PDTC-treated group was compared with the obese *db/db* group.

### 3.7 OONO<sup>-</sup> production and 3-NT immunofluorescence

Untreated obese *db/db* mice had significantly higher OONO<sup>-</sup> production rates as determined by EPR, and significantly higher protein expression of 3-NT, an indicator of OONO<sup>-</sup> production (Figure 2E and F). PDTC treatment significantly attenuated OONO<sup>-</sup> production and 3-NT expression in *db/db* mice, normalizing levels to those of lean controls.

### 3.8 Mitochondrial purity and swelling assay

Mitochondrial purity as determined by TEM and western blot for the mitochondrial markers ANT and VDAC (Figure 3A and B). The functional integrity of the mitochondria was assessed by the

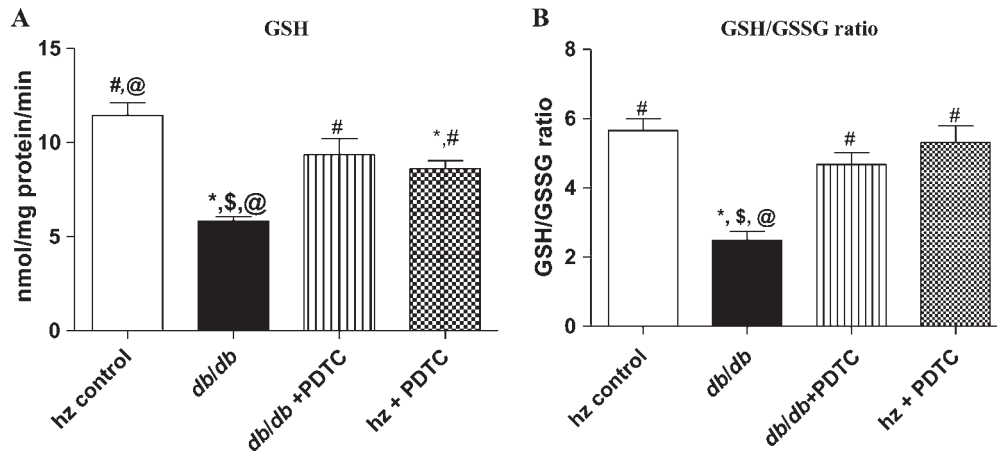


**Figure 1** (A) Mean GSH levels for each experimental group as determined by a kit method. (B) Mean GSH/GSSG ratios for each experimental group. Note the marked decrease in GSH levels and GSH/GSSG ratio for the *db/db* group and the normalization of these parameters by PDTC treatment. \* $P < 0.05$  vs. control; # $P < 0.05$  vs. *db/db*; \$ $P < 0.05$  vs. *db/db* PDTC; @ $P < 0.05$  vs. hz PDTC.

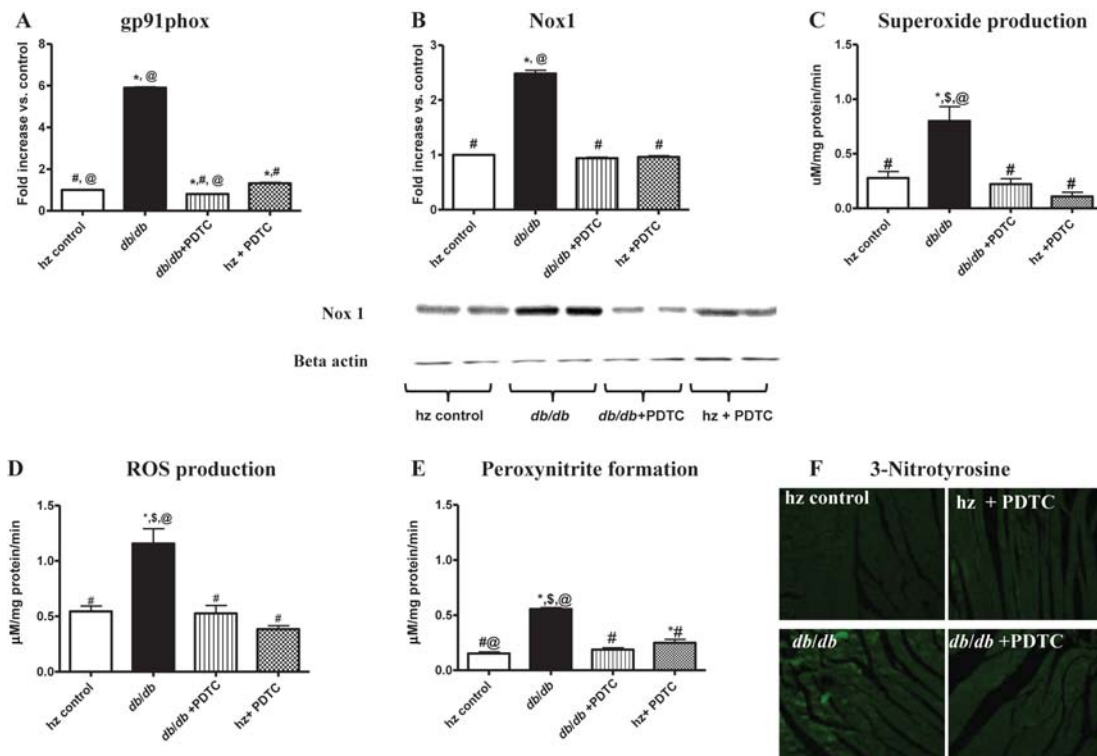


**Figure 2** Gene expression levels of (A) gp91phox and (B) Nox1 as determined by real-time RT-PCR and western blotting. Both of these genes were significantly upregulated in *db/db* LV tissue, and PDTC treatment attenuated expression of these genes. Production levels of (C) superoxide, (D) total ROS, and (E) peroxynitrite as determined by EPR spectroscopy. Levels of superoxide, total ROS, and peroxynitrite production were all increased significantly in *db/db* LV tissue; these levels were normalized with PDTC treatment. (F) Protein expression levels of 3-nitrotyrosine in LV tissues from all experimental groups. \* $P < 0.05$  vs. control; # $P < 0.05$  vs. *db/db*; \$ $P < 0.05$  vs. *db/db* PDTC; @ $P < 0.05$  vs. hz PDTC.



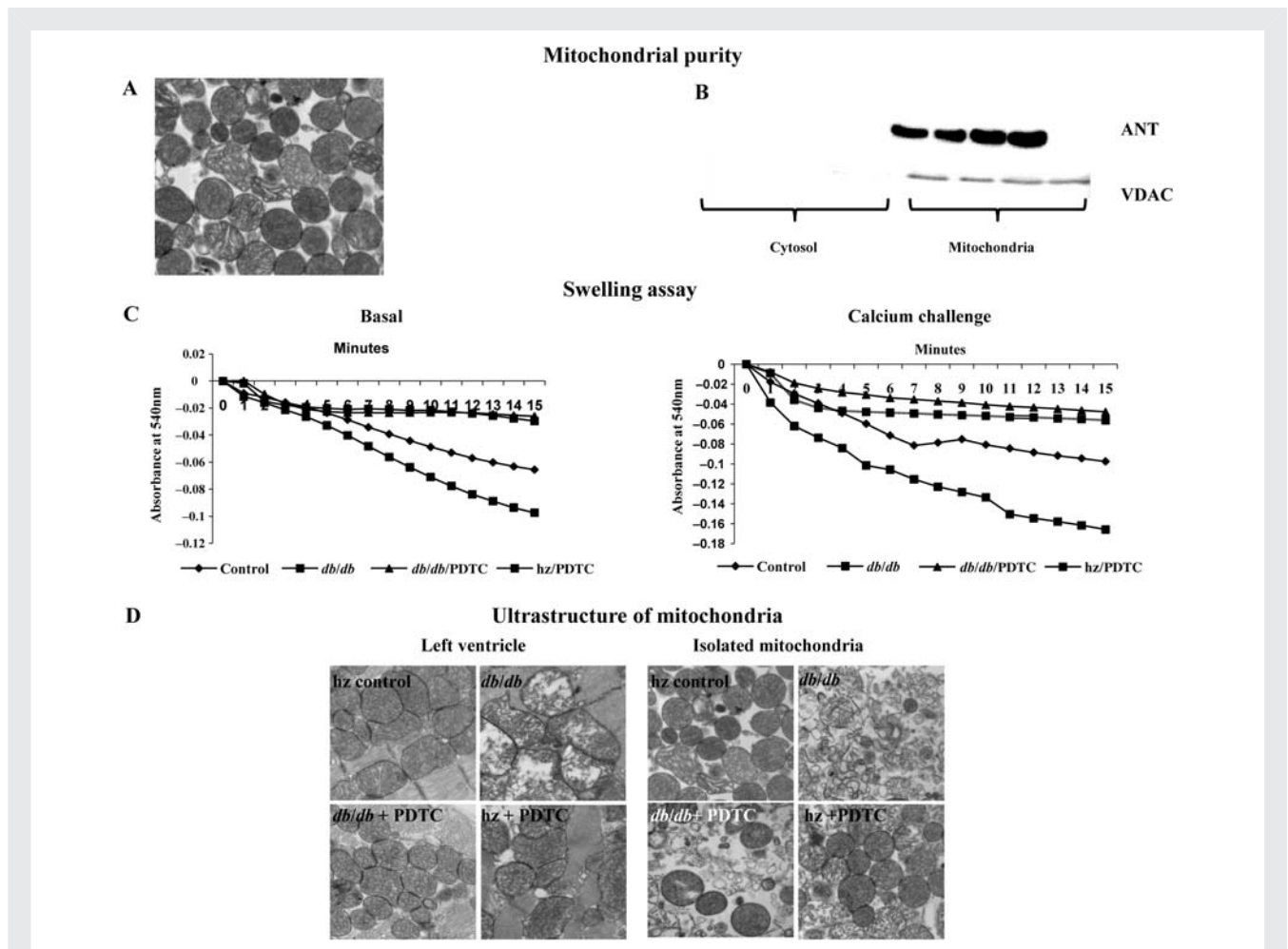


**Figure 3** (A and B) Mitochondrial purity as determined by transmission electron microscopy (TEM) and western blot for the mitochondrial markers ANT and VDAC. (C) Results from swelling assay presented in graphical form. (D) Ultrastructural changes of LV tissue and isolated LV mitochondria as examined with TEM; ( $\times 40$  magnification). Note the disordered appearance of the mitochondria and lack of cristae in *db/db* animals, and the preservation of appearance with PDTC treatment.

evaluation of permeability transition (swelling assay). When compared with controls, obese *db/db* mice had increased swelling both at the basal level and in the presence of a calcium challenge, indicating mitochondrial damage (Figure 3C). In contrast, mitochondria from the *db/db* obese + PDTC and *hz* + PDTC treatment groups showed maintenance of structural and functional integrity when compared with mitochondria from the *db/db* obese group.

### 3.9 Ultrastructure of LV tissue and mitochondria

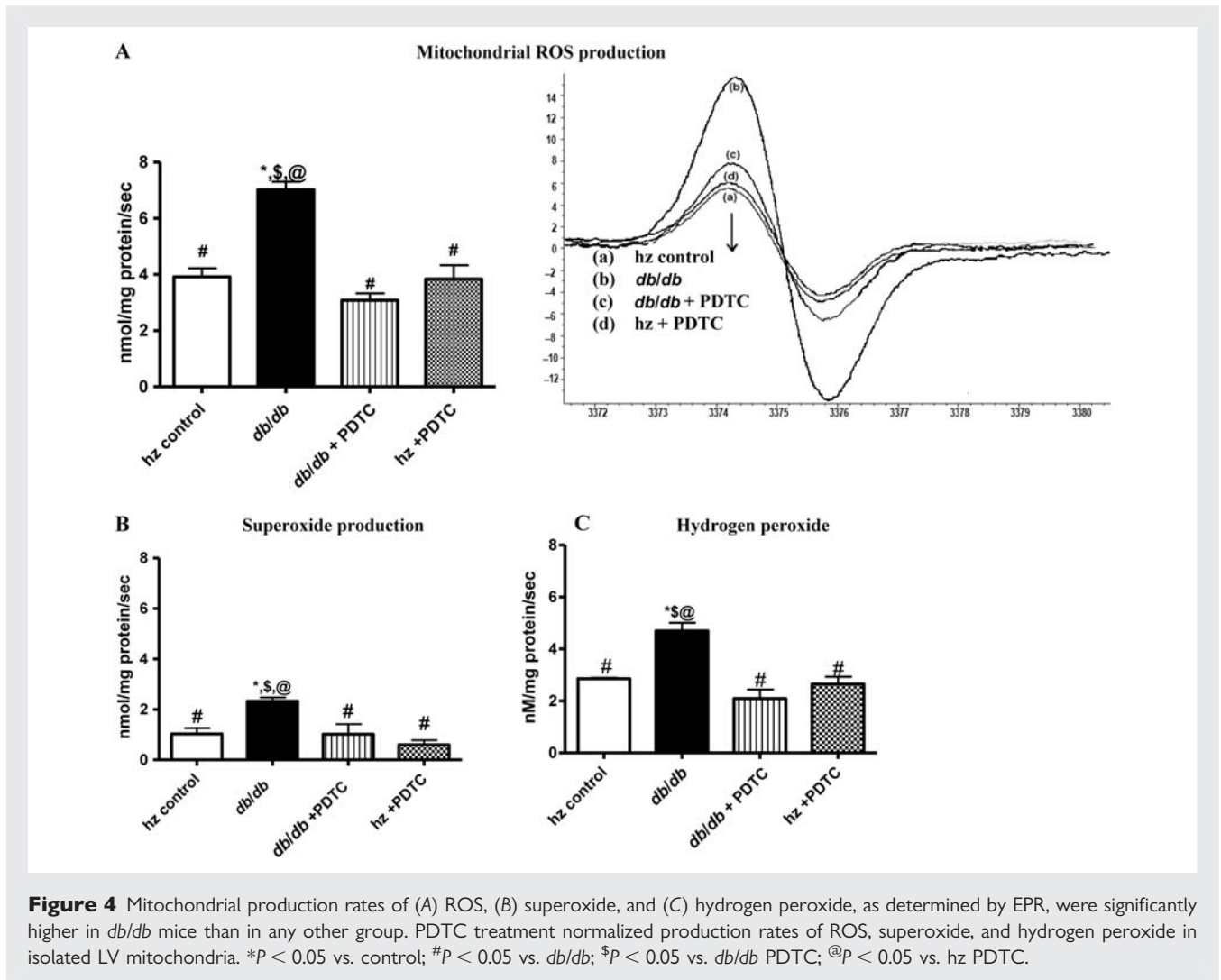
The ultrastructural changes of LV tissue and mitochondria are shown in Figure 3D. The LV and isolated mitochondria of *hz* controls appeared normal in structure and architecture, with visible inner and outer membranes and regular arrangement of cristae. The mitochondria from untreated obese *db/db* mice were characterized by numerous vesicular cristae with membrane rupture. PDTC treatment protected from alterations of inner membrane integrity in the mitochondria of *db/db* mice.

### 3.10 Mitochondrial ROS, $O_2^{\bullet-}$ , and $H_2O_2$ production

Total ROS,  $O_2^{\bullet-}$ , and  $H_2O_2$  production rates in mitochondria, as determined by EPR, were all significantly higher in LV mitochondria of untreated obese *db/db* mice than in *hz* controls, *db/db* + PDTC, and *hz* + PDTC animals (Figure 4A–C). These findings suggest that increased mitochondrial oxidative stress induced by NF- $\kappa$ B contributes to mitochondrial dysfunction.

### 3.11 Mitochondrial complex III activity

We chose to focus on complex III in this study because it is the major complex in the ETC and is a major site of  $O_2^{\bullet-}$  production. Complex III activity was significantly decreased in obese *db/db* mice relative to controls (Figure 5A). Significant decreases in mitochondrial complex III activity were observed in the obese *db/db* group when compared with the activities of the PDTC-treated obese *db/db* mice and controls ( $P < 0.05$ ).



### 3.12 ATP/ADP ratio

Significant decreases in ATP levels were found in the untreated obese *db/db* group when compared with hz control, *db/db* + PDTC, and hz + PDTC animals (Figure 5B). No significant differences in ATP levels were found among other groups. Similar trends were seen in ATP/ADP ratios (Figure 5C). Collectively, these data suggest a role for NF- $\kappa$ B in the oxidative stress and mitochondrial dysfunction seen in the diabetic condition.

### 3.13 NF- $\kappa$ B p65 activity

NF- $\kappa$ B p65 subunit activity was significantly elevated in the hearts of *db/db* animals (Figure 6A). PDTC treatment significantly reduced ROS-induced NF- $\kappa$ B p65 activity in the nuclear fractions of obese *db/db* mice, restoring activity levels to values near those of hz control, hz + PDTC, and *db/db* + PDTC animals.

### 3.14 NF- $\kappa$ B p50 gene expression

Expression levels of p50, as determined by real-time RT-PCR, were significantly higher in obese *db/db* mice than in hz controls (Figure 6B;  $P < 0.05$ ). Treatment with PDTC partially attenuated, but did not normalize, p50 gene expression in *db/db* mice.

### 3.15 Mitochondrial NF- $\kappa$ B p50 protein levels

Protein expression levels of p50 in isolated LV mitochondria were significantly higher in obese *db/db* mice than in control lean mice. PDTC treatment partially attenuated mitochondrial p50 expression in *db/db* mice. A representative western blot is shown in Figure 6C.

## 4. Discussion

The novel findings of the current study are that NF- $\kappa$ B p50 is increased in the mitochondria of obese *db/db* mice and is associated with increased oxidative stress and that blockade of NF- $\kappa$ B in obese mice protects the heart against oxidative stress, restores mitochondrial integrity, and improves cardiac function. These results suggest that NF- $\kappa$ B contributes to end-organ damage in type II DM.

Cytosolic NF- $\kappa$ B p50 gene expression and NF- $\kappa$ B p65 activity (ELISA) were measured to determine whether PDTC was actually blocking NF- $\kappa$ B activity. Animals with diabetes had increased NF- $\kappa$ B p50 gene expression and NF- $\kappa$ B p65 activity; these

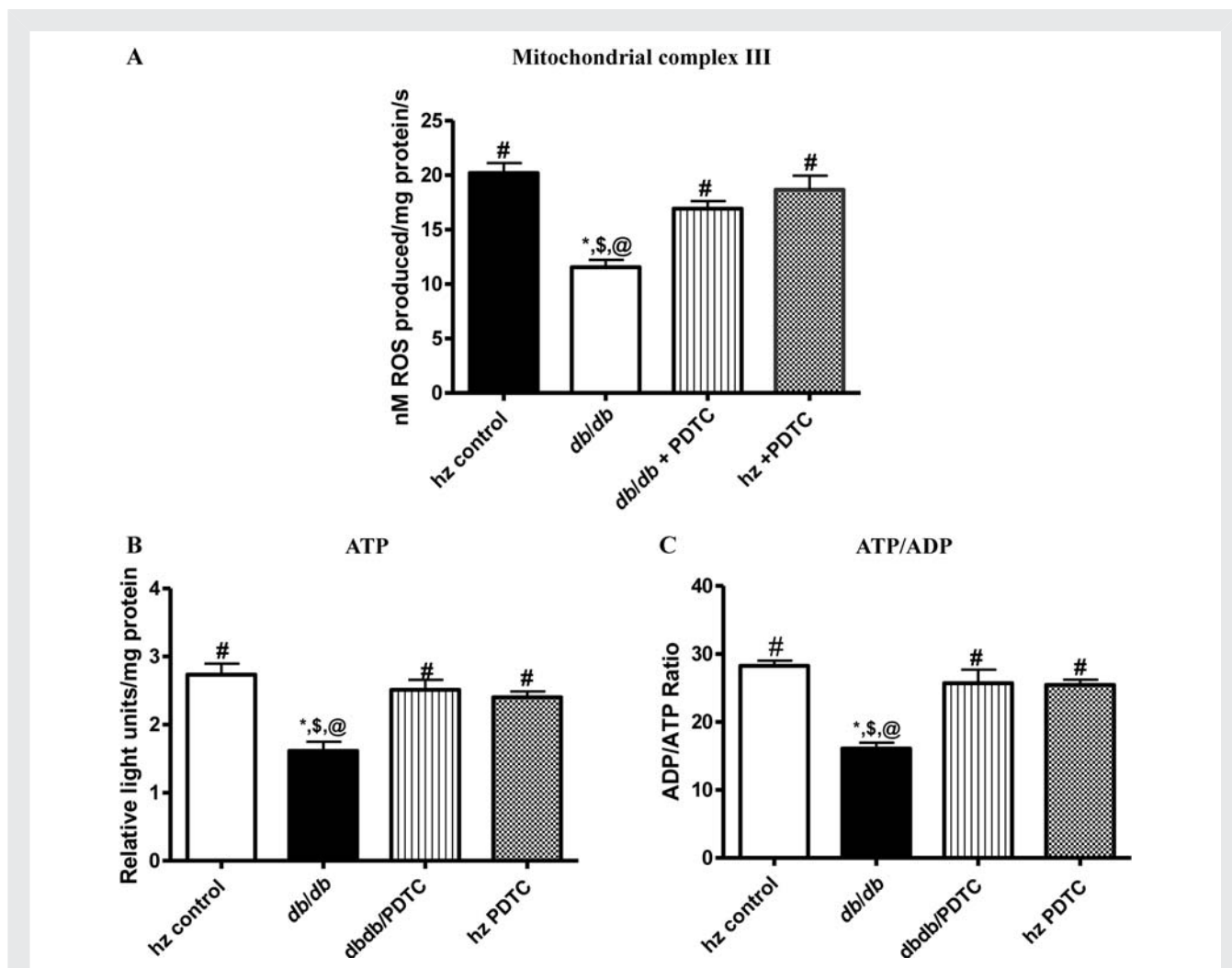


**Figure 5** (A) Mitochondrial complex III activity as determined by EPR, (B) ATP production, and (C) ATP/ADP ratios were all decreased in *db/db* animals when compared with other groups. Treatment with PDTC restored mitochondrial complex III activity and ATP production and improved ATP/ADP ratio. \* $P < 0.05$  vs. control; # $P < 0.05$  vs. *db/db*; \$ $P < 0.05$  vs. *db/db* PDTC; @ $P < 0.05$  vs. hz PDTC.

changes were prevented in *db/db* + PDTC mice. Since NF- $\kappa$ B responds to and induces oxidative stress,<sup>17,18</sup> we also measured GSH and GSH/GSSG ratio in these animals. We found a decrease in GSH and GSH/GSSG in obese *db/db* animals; these results indicate an impaired antioxidant status in the diabetic condition. Treatment with PDTC prevented these changes. We believe that the effects PDTC seen in this study may be due to a combination effect, with both the ROS scavenging and NF- $\kappa$ B inhibiting properties playing roles. Further experiments must be performed to elucidate the exact mechanism under which PDTC provides the protective effects seen in our study. Overall, these results highlight the negative effect of NF- $\kappa$ B on the antioxidant defence mechanism of diabetic LV tissue and strongly suggest a role for NF- $\kappa$ B in diabetes-induced oxidative stress.

Diabetes is associated with a chronic inflammatory state characterized by increased circulating levels of PIC (TNF, IL-6) and contributes to the pathophysiology of cardiovascular disease.<sup>32</sup> TNF- $\alpha$  and IL-6 have been shown to increase concentrations of plasma

triglycerides and VLDL-c. This suggests that improvements in blood cholesterol and triglyceride levels could be due, in part, to reduced TNF- $\alpha$  and/or IL-6 levels in obese *db/db* mice treated with PDTC.

We also examined the effect of PDTC treatment on the expression of gp91phox and its homologue, Nox1. In obese *db/db* mice, expression levels of both genes were increased, indicating increases in diabetes-mediated oxidative stress. PDTC treatment decreased expression of these genes, again suggesting an involvement of NF- $\kappa$ B in diabetes. Alterations in gp91phox and Nox1 protein expression were further confirmed by measuring ROS and  $O_2^{\bullet-}$  production using EPR. The 3-NT formation seen in our study was likely a result of overproduction of superoxide in the diabetic heart, which in turn reacts with NO to produce peroxynitrite, the causative agent for the formation of 3-NT. Evidence that the increased superoxide was responsible for the formation of 3-NT was supported by the fact that suppression of superoxide formation resulted in reduced formation of 3-NT.



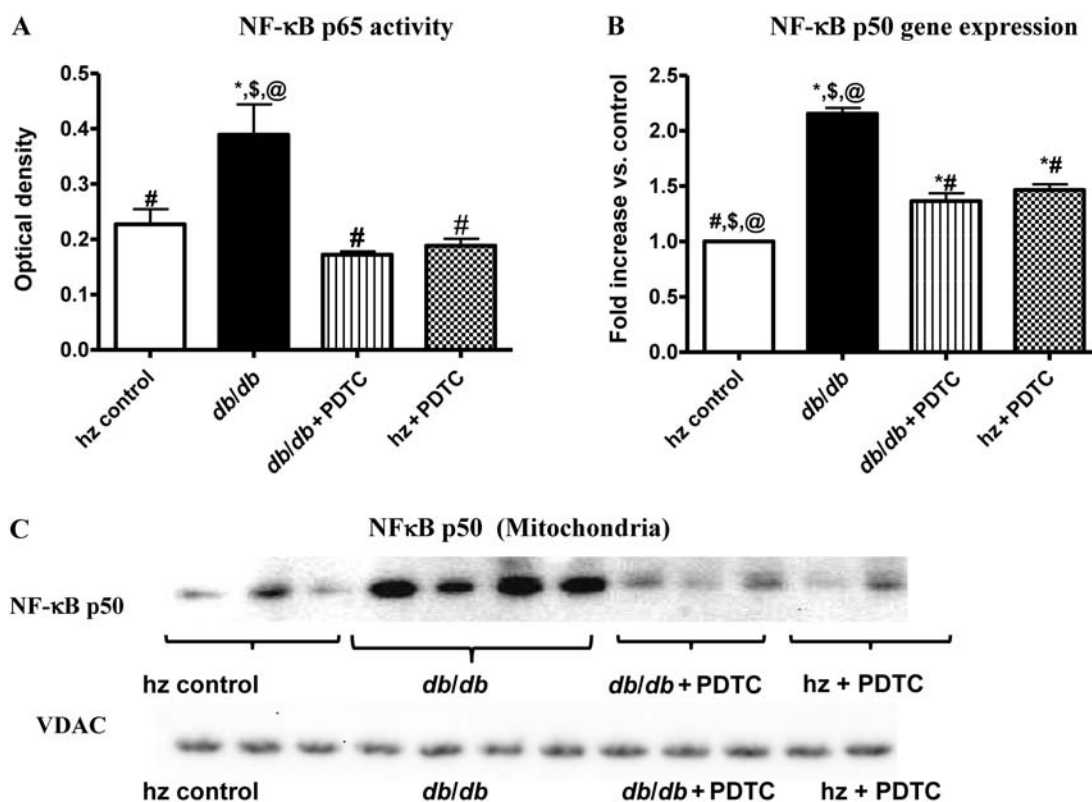


**Figure 6** (A) NF-κB p65 activity as determined by ELISA was significantly higher in *db/db* mice and was attenuated with PDTC treatment. (B) Tissue gene expression and (C) mitochondrial protein expression of NF-κB p50 (as determined by real-time RT-PCR and western blot, respectively) were significantly higher in *db/db* animals; this expression was attenuated, but not normalized, with PDTC treatment. \* $P < 0.05$  vs. control; # $P < 0.05$  vs. *db/db*; \$ $P < 0.05$  vs. *db/db* PDTC; @  $< 0.05$  vs. hz PDTC.

Recent studies have demonstrated that oxidative damage induced by ROS and reactive nitrogen species derived from hyperglycaemia plays a critical role in diabetic injury in multiple organs.<sup>33</sup> In this study, we saw increases in production of total ROS, superoxide, and peroxynitrite in diabetic animals. Furthermore, in some pathological cases, excess superoxide anion can interact with NO, which is produced physiologically by constitutive sources, such as the endothelial isoform of NO synthase.<sup>34,35</sup> This process results in the formation of the strong oxidant peroxynitrite, which reacts with various biomolecules and leads to the production of the modified amino acid, nitrotyrosine.<sup>36,37</sup> In this paper, we have demonstrated a role for nitrosative stress, particularly that of the peroxynitrite molecule, in the pathogenesis of diabetic complications. These results are consistent with those obtained from heart tissue from mouse and rat models.<sup>38,39</sup>

Mitochondria are a major source of ROS production.<sup>40</sup> We recently demonstrated that chronic TNF administration induced mitochondrial damage by altering mitochondrial respiration and decreasing ATP production. In a recent related study, we demonstrated that NF-κB blockade protects against renal cortical mitochondrial damage.<sup>20</sup> Since NF-κB contributes to oxidative stress, we next wanted to examine the role played by NF-κB on mitochondrial oxidative stress in diabetic animals. Here, we examined whether NF-κB itself is increased in the mitochondria, to cause

an increase in ROS production within the mitochondria. Our results are the first to demonstrate that NF-κB p50 expression is increased in the cardiac mitochondria of *db/db* mice and that treatment with PDTC protects against mitochondrial damage (Figure 6C). These findings suggest that in diabetes, inflammatory cytokines or their transcription factor, NF-κB, enter into the mitochondria to increase oxidative stress and cause cardiac dysfunction. However, the underlying mechanisms by which NF-κB can enter the mitochondrion are unclear and require further investigation.

It has been suggested that increased mitochondrial ROS production during hyperglycaemia is central to diabetic complications.<sup>41,42</sup> Therefore, increases in mitochondrial ROS, superoxide, and hydrogen peroxide production and oxidative damage may contribute to the onset, progression, and pathological consequences of type II diabetes. A number of functional enzymes within the mitochondria are particularly susceptible to ROS-mediated damage, leading to altered ATP synthesis, electron transport dysregulation, and induction of mitochondrial membrane permeability, all of which predispose to cardiac dysfunction. The possibility of a role for mitochondria in the development of diabetic cardiac disease is further strengthened by our findings regarding mitochondrial complex III activity, ATP levels, and ATP/ADP ratio. Increased ROS production was evident in the hearts of obese *db/db* mice, and likely affected the mitochondrial ETC

system by promoting mitochondrial uncoupling, as evidenced by increased ROS production, reduced ATP/ADP ratio, and decreased mitochondrial complex III activity. Impairment of complex III activity due to NF- $\kappa$ B-induced oxidative damage may increase electron leak from the ETC, thereby generating more superoxide and perpetuating a cycle of oxygen radical-induced damage to the diabetic heart. In addition to impairing mitochondrial coupling,<sup>43</sup> ROS can also oxidize lipids and proteins and other intracellular molecules (such as NO) to produce highly reactive products, which damage the cell.<sup>44</sup> Decreased ATP production was also associated with a worsening of cardiac function as exhibited by a reduction in FS% and increases in LVD and LVS in the untreated obese *db/db* group. In contrast, NF- $\kappa$ B blockade reduced mitochondrial damage, restored ATP production rates, and normalized FS% and Tei index. These findings suggest that NF- $\kappa$ B contributes to mitochondrial damage, partly by decreasing ATP production and leads to altered cardiac function in this mouse model of type II diabetes.

In conclusion, the major findings of our study are: (i) NF- $\kappa$ B gene and protein expressions are increased in the mitochondria and contribute to enhanced oxidative stress and (ii) treatment with NF- $\kappa$ B blockers attenuates mitochondrial oxidative stress and protects against cardiac dysfunction through modulation of cardiac NF- $\kappa$ B activity. These findings suggest that NF- $\kappa$ B might be an important molecule contributing to end-organ damage in type II diabetes.

## Supplementary material

Supplementary material is available at *Cardiovascular Research* online.

## Acknowledgements

The authors thank Sherry Ring for sectioning the tissue samples.

**Conflict of interest:** none declared.

## Funding

These studies were supported by a grant from the National Heart Lung and Blood Institute (RO1 HL080544-01) for J.F.

## References

1. NIDDK. National Diabetes Statistics, 2007. Bethesda, MD: US Department of Health and Human Services, NIH; 2008.
2. AHA. *Metabolic Syndrome Statistics Statistical Fact Sheets*. Dallas, TX: American Heart Association; 2009.
3. Kelishadi R, Gharipour M, Sadri GH, Tavasoli AA, Amani A. Cardiovascular disease risk factors, metabolic syndrome and obesity in an Iranian population. *East Mediterr Health J* 2008;**14**:1070–1079.
4. Khan KA, Sowers JR. Surgical treatment of the cardiometabolic syndrome and obesity. *J Cardiometab Syndr* 2008;**3**:254–257.
5. Cai L, Kang YJ. Oxidative stress and diabetic cardiomyopathy: a brief review. *Cardiovasc Toxicol* 2001;**1**:181–193.
6. Lopes JP, Oliveira SM, Soares Fortunato J. Oxidative stress and its effects on insulin resistance and pancreatic beta-cells dysfunction: relationship with type 2 diabetes mellitus complications. *Acta Med Port* 2008;**21**:293–302.
7. Pop-Busui R, Sima A, Stevens M. Diabetic neuropathy and oxidative stress. *Diabetes Metab Res Rev* 2006;**22**:257–273.
8. Ziolo MT, Kohr MJ, Wang H. Nitric oxide signaling and the regulation of myocardial function. *J Mol Cell Cardiol* 2008;**45**:625–632.

9. Ungvari Z. Role of Oxidative-nitrosative stress and downstream pathways in various forms of cardiomyopathy and heart failure. *Curr Vasc Pharmacol* 2005;**3**: 221–229.
10. Szabo C. Multiple pathways of peroxynitrite cytotoxicity. *Toxicol Lett* 2003;**140–141**:113–124.
11. Turko IV, Murad F. Protein nitration in cardiovascular diseases. *Pharmacol Rev* 2002;**54**:619–634.
12. Hausladen A, Fridovich I. Superoxide and peroxynitrite inactivate aconitases, but nitric oxide does not. *J Biol Chem* 1994;**269**:29405–29408.
13. Sriramula S, Haque M, Majid DS, Francis J. Involvement of tumor necrosis factor- $\alpha$  in angiotensin II-mediated effects on salt appetite, hypertension, and cardiac hypertrophy. *Hypertension* 2008;**51**:1345–1351.
14. Kang YM, Ma Y, Elks C, Zheng JP, Yang ZM, Francis J. Cross-talk between cytokines and renin-angiotensin in hypothalamic paraventricular nucleus in heart failure: role of nuclear factor- $\kappa$ B. *Cardiovasc Res* 2008;**79**:671–678.
15. Mariappan N, Soorappan RN, Haque M, Sriramula S, Francis J. TNF- $\alpha$ -induced mitochondrial oxidative stress and cardiac dysfunction: restoration by superoxide dismutase mimetic Tempol. *Am J Physiol Heart Circ Physiol* 2007;**293**: H2726–H2737.
16. Mariappan N, Elks CM, Fink B, Francis J. TNF-induced mitochondrial damage: a link between mitochondrial complex I activity and left ventricular dysfunction. *Free Radic Biol Med* 2009;**46**:462–470.
17. Schreck R, Albermann K, Baeuerle PA. Nuclear factor  $\kappa$ B: an oxidative stress-responsive transcription factor of eukaryotic cells (A review). *Free Radic Res Commun* 1992;**17**:221–237.
18. Schreck R, Rieber P, Baeuerle PA. Reactive oxygen intermediates as apparently widely used messengers in the activation of the NF- $\kappa$ B transcription factor and HIV-1. *EMBO J* 1991;**10**:2247–2258.
19. Christman JW, Blackwell TS, Juurlink BH. Redox regulation of nuclear factor  $\kappa$ B: therapeutic potential for attenuating inflammatory responses. *Brain Pathol* 2000;**10**:153–162.
20. Elks CM, Mariappan N, Haque M, Guggilam A, Majid DS, Francis J. Chronic NF- $\kappa$ B blockade reduces cytosolic and mitochondrial oxidative stress and attenuates renal injury and hypertension in SHR. *Am J Physiol Renal Physiol* 2009;**296**:F298–F305.
21. Ebenezer PJ, Mariappan N, Elks CM, Haque M, Soltani Z, Reisin E et al. Effects of pyrrolidine dithiocarbamate on high-fat diet-induced metabolic and renal alterations in rats. *Life Sci* 2009;**85**:357–364.
22. Brennan P, O'Neill LA. Inhibition of nuclear factor  $\kappa$ B by direct modification in whole cells—mechanism of action of nordihydroguaiaric acid, curcumin and thiol modifiers. *Biochem Pharmacol* 1998;**55**:965–973.
23. Brennan P, O'Neill LA. Inhibition of NF  $\kappa$ B activity by oxidative processes in intact cells mechanism of action of pyrrolidine dithiocarbamate and diamide. *Biochem Soc Trans* 1996;**24**:3S.
24. Bowie A, O'Neill LAJ. Oxidative stress and nuclear factor- $\kappa$ B activation: a reassessment of the evidence in the light of recent discoveries. *Biochem Pharmacol* 2000;**59**:13–23.
25. Staal FJT, Roederer M, Herzenberg LA. Intracellular thiols regulate activation of nuclear factor  $\kappa$ B and transcription of human immunodeficiency virus. *Proc Natl Acad Sci USA* 1990;**87**:9943–9947.
26. Zimmerman MC, Zucker IH. Mitochondrial dysfunction and mitochondrial-produced reactive oxygen species: new targets for neurogenic hypertension? *Hypertension* 2009;**53**:112–114.
27. Tsutsui H. Oxidative stress in heart failure: the role of mitochondria. *Intern Med* 2001;**40**:1177–1182.
28. Brownlee M. The pathobiology of diabetic complications. *Diabetes* 2005;**54**: 1615–1625.
29. Brownlee M. Biochemistry and molecular cell biology of diabetic complications. *Nature* 2001;**414**:813–820.
30. Sriramula S, Haque M, Majid DSA, Francis J. Involvement of tumor necrosis factor- $\alpha$  in angiotensin II-mediated effects on salt appetite, hypertension, and cardiac hypertrophy. *Hypertension* 2008;**51**:1345–1351.
31. Khaleduzzaman M, Francis J, Corbin ME, McIlwain E, Boudreaux M, Du M et al. Infection of cardiomyocytes and induction of left ventricle dysfunction by neurovirulent polytropic murine retrovirus. *J Virol* 2007;**81**:12307–12315.
32. Van Gaal LF, Mertens IL, De Block CE. Mechanisms linking obesity with cardiovascular disease. *Nature* 2006;**444**:875–880.
33. Pachter P, Beckman JS, Liaudet L. Nitric oxide and peroxynitrite in health and disease. *Physiol Rev* 2007;**87**:315–424.
34. Onozato ML, Tojo A, Goto A, Fujita T, Wilcox CS. Oxidative stress and nitric oxide synthase in rat diabetic nephropathy: effects of ACEI and ARB. *Kidney Int* 2002;**61**:186–194.
35. Lyall F, Gibson JL, Greer IA, Brockman DE, Eis AL, Myatt L. Increased nitrotyrosine in the diabetic placenta: evidence for oxidative stress. *Diabetes Care* 1998;**21**: 1753–1758.

36. Ceriello A, Quagliaro L, Catone B, Pascon R, Piazzola M, Bais B et al. Role of hyperglycemia in nitrotyrosine postprandial generation. *Diabetes Care* 2002;**25**:1439–1443.
37. Pacher P, Obrosova IG, Mabley JG, Szabo C. Role of nitrosative stress and peroxynitrite in the pathogenesis of diabetic complications. Emerging new therapeutical strategies. *Curr Med Chem* 2005;**12**:267–275.
38. Cai L, Wang J, Li Y, Sun X, Wang L, Zhou Z et al. Inhibition of superoxide generation and associated nitrosative damage is involved in metallothionein prevention of diabetic cardiomyopathy. *Diabetes* 2005;**54**:1829–1837.
39. Ceriello A, Quagliaro L, D'Amico M, Di Filippo C, Marfella R, Nappo F et al. Acute hyperglycemia induces nitrotyrosine formation and apoptosis in perfused heart from rat. *Diabetes* 2002;**51**:1076–1082.
40. Chen Q, Lesnfsky EJ. Depletion of cardiolipin and cytochrome c during ischemia increases hydrogen peroxide production from the electron transport chain. *Free Radic Biol Med* 2006;**40**:976–982.
41. Nishikawa T, Edelstein D, Du XL, Yamagishi S, Matsumura T, Kaneda Y et al. Normalizing mitochondrial superoxide production blocks three pathways of hyperglycaemic damage. *Nature* 2000;**404**:787–790.
42. Du XL, Edelstein D, Rossetti L, Fantus IG, Goldberg H, Ziyadeh F et al. Hyperglycemia-induced mitochondrial superoxide overproduction activates the hexosamine pathway and induces plasminogen activator inhibitor-1 expression by increasing Sp1 glycosylation. *Proc Natl Acad Sci USA* 2000;**97**:12222–12226.
43. Echtay KS, Roussel D, St-Pierre J, Jekabsons MB, Cadenas S, Stuart JA et al. Superoxide activates mitochondrial uncoupling proteins. *Nature* 2002;**415**:96–99.
44. Ceylan-Isik AF, Wu S, Li Q, Li SY, Ren J. High-dose benfotiamine rescues cardiomyocyte contractile dysfunction in streptozotocin-induced diabetes mellitus. *J Appl Physiol* 2006;**100**:150–156.